

# Designing laterally loaded piles relying on the Generalized Coefficient of Earth Pressure and static analysis of elastic beams

Lysandros Pantelidis (✉ [lysandros.pantelidis@cut.ac.cy](mailto:lysandros.pantelidis@cut.ac.cy))

Cyprus University of Technology <https://orcid.org/0000-0001-5979-6937>

---

## Research Article

**Keywords:** laterally loaded piles, the Generalized Coefficient of Earth Pressure, static analysis of elastic beams, intermediate earth pressures, p-y method

**DOI:** <https://doi.org/10.21203/rs.3.rs-2666388/v1>

**License:** © ⓘ This work is licensed under a Creative Commons Attribution 4.0 International License.

[Read Full License](#)

---

# Designing laterally loaded piles relying on the Generalized Coefficient of Earth Pressure and static analysis of elastic beams

Lysandros Pantelidis<sup>1,\*</sup>

<sup>1</sup> Cyprus University of Technology, 3036 Limassol, CY

\* [lysandros.pantelidis@cut.ac.cy](mailto:lysandros.pantelidis@cut.ac.cy)

## Abstract

There is no doubt that the problem of a laterally loaded pile is an earth pressure analysis problem, involving the flexural rigidity of the pile and the possible fixity of the pile head to a pile cap. During the deformation, which is a combination of bending, rotation and horizontal translation, the earth pressures may take any value between the state at-rest and the active or the passive state on the two sides of the pile. The current practice, as this is depicted by the various design standards, is the  $p - y$  method, with the soil to be replaced by an array of parallel springs. This simplification is accompanied by rough assumptions for the Winkler spring constant. Relatively, the author offers a brief, yet comprehensive, review of the more important  $p - y$  methods, shedding some light to their validity and highlighting the need for adopting a more rational approach. In this respect, quite recently the author proposed a continuum mechanics approach for deriving earth pressure coefficients for any soil state between the at-rest state and the active or the passive state, applicable to cohesive-frictional soils and both horizontal and vertical pseudo-static conditions. An analytical expression for the calculation of the required structure movement for the mobilization of the active or passive failure state of soil is also provided. The proposed method combines these expressions with the static analysis of elastic beams, offering complete earth pressure and pile deflection diagrams, taking also into account the inertial effect of a possible seismic event (in a pseudostatic manner), as well as the overconsolidation caused by a displacement pile to the surrounding soil. Finally, the location of the point of virtual fixity, which is an important parameter in the case of long, slender piles, is calculated following the proposed procedure.

**Keywords:** laterally loaded piles; the Generalized Coefficient of Earth Pressure; static analysis of elastic beams; intermediate earth pressures;  $p - y$  method

## 1 Introduction

Pile foundations are commonly used in major projects (e.g., high-rise buildings, bridges, offshore structures) to withstand large axial and lateral loads. Assessing piles subjected to lateral loads is, however, a rather difficult task. Already from the middle of the previous century, a great number of methods has been proposed. The methods included, however, in a design standard are supposed to reflect the best current practice; thus, in this paper, the author will focus on what EN1997-1:2004 [1], prEN1997-3:2022 [2] (draft standard), American Petroleum Institute (API) [3], FHWA [4] and AASHTO [5] foresee for this type of loading on piles. These methods are briefly reviewed in the following section.

The problem of a lateral loaded pile is, essentially, an earth pressure analysis problem, involving all soil states and especially the intermediate ones, both on the active and the passive “sides”. Intermediate values of earth pressure occur if the pile movement is insufficient to mobilize the active or passive limiting values. In this respect, the author [6] proposed in 2019 a continuum mechanics approach for deriving earth pressure coefficients for any soil state between the at-rest state and the active or passive state, applicable to cohesive-frictional soils and both horizontal and vertical pseudo-static conditions (see also [7–9]). The same method also provides analytical expression for the calculation of the required pile movement  $\Delta y_{max}$  for the mobilization of the active or passive failure state. The basic expressions are summarized in Section 3, while the proposed method for the analysis of laterally loaded piles combines these expressions with the static analysis of elastic beams.

## 2 A brief review of the methods adopted by various important design standards

This section is dedicated to the five design standards mentioned in the introduction, EN1997-1:2004 [1], prEN1997-3:2022 [2], API [3], FHWA [4] and AASHTO [5].

FHWA [4] and AASHTO [5] make a simple reference to Broms’ [11] hand calculation method for both cohesive and cohesionless soils, while they rather prompt to the use of Reese’s computer solution [12, 13]. Besides FHWA [4] mentions that, as lateral load demand has increased along with the need for improved deformation estimates more detailed load-deformation computer analyses have become the norm. Reese’s method is discussed later, as part of

a general discussion for the  $p - y$  method. Regarding Broms' method, Russo and Viggiani [14, 15] checked the method in question by means of a database including over 50 horizontal load tests on piles taken to failure and sufficiently well documented to allow a back analysis of the results. Their comparison analysis shows that the vast majority of data points fall within the  $\pm 40\%$  confidence lines, symmetrically for both clays and sands, although a cloud of points lies outside the  $-40\%$  confidence line (conservative side) for the case of sands.

EN1997-1:2004 highlights the need for considering the compatibility of strains in the analysis of laterally loaded piles (§2.4.1(13)), indicating that numerical methods can be appropriate if compatibility of strains or the interaction between the structure and the soil at a limit state are considered (§2.4.1(12)). "Numerical methods" may refer to three-dimensional finite element analysis or, rather, to the  $p - y$  method, as for "long slender piles" EN1997-1:2004 makes a clear reference to the theory of a beam loaded at the top and supported by a deformable medium characterized by a horizontal modulus of subgrade reaction (§7.7.3(3)). And despite the fact that, EN1997-1:2004 (§7.7.1(3)) discretizes the piles to "short" and "long slender" ones, the standard in question does not suggest a specific method, not even a general design framework for "short" piles; "short" piles are subjected to rotation or translation as a rigid body, while "long slender" ones are subjected to bending failure of the pile, accompanied by local yielding and displacement of the soil near the top of the pile. prEN1997-3:2022 (§6.5.4(2)), on the other hand, is more specific about what "short" and "longer" (as it calls them) piles are, discretizing them by the length ( $L$ ) to diameter ( $D$ ) ratio. More specifically, piles with  $L/D < 6$  are considered to be "short", while piles with  $L/D \geq 6$  are considered to be "longer". It also mentions that the transverse resistance of a single pile "*shall*" take account of the fixity of the pile head to the pile cap or sub-structure and the fixity of the pile base (§6.5.4(4)), apparently because these two restrictions make the pile to behave differently under lateral loading. The word "*shall*" impose an obligation or a requirement [16], however, prEN1997-3:2022 does not suggest a method which take account of the fixity of the pile head to the pile cap; the other methods mentioned in this paper also do not include such a method. Moreover, the draft standard prEN1997-3:2022 seems to largely rely on the  $p - y$  method, suggesting in "Annex C12" (denoted as "informative") a calculation model for the lateral displacement of single pile using load transfer functions.

Referring to the  $p - y$  method, this is, probably, the most widely used method for calculating the response of “long” piles under lateral loading; Matlock’s [17], Reese et al. [18], O’Neill and Murchison’s [19, 20] and Brinch-Hansen’s [21] methods for soft clays, stiff clays, sands and general  $c' - \varphi'$  soils respectively are among the most popular ones. Indeed, the first three of them (published in 1970, 1975 and 1983 respectively) are included in American Petroleum Institute (API) [3] standard, while the Brinch-Hansen method (published in 1961) in prEN1997-3:2022. For the case of clays, prEN1997-3:2022 suggests a variation of Matlock’s [17] method. More specifically, prEN1997-3:2022 (Annex C12) suggests that the behaviour of transversally loaded piles be considered by the following bilinear (elastic – perfectly plastic) model:

$$p = \min\left(\frac{p_f}{y_f} \cdot y; p_f\right) \quad (1)$$

where,  $p_f$  is the lateral pressure of the ground at failure,  $p$  is the lateral pressure and  $y_f$  is the transversal deflection of the pile. The latter takes the default value of  $0.1D$ ,  $0.12D$  or  $0.05D$  for coarse soils, fine soils under long-term loading or fine soils under short-term loading respectively; these, however, are only rough estimates and not case-specific values. Thus, any error in  $y_f$ , which may be very high if the default value deviates greatly from the actual value, is directly transferred to  $p$  through Equation 1. Regarding  $p_f$ , prEN1997-3:2022 has adopted the Brinch-Hansen’s [21] method for drained soil conditions and the  $p_{fd} = 9 \cdot c_{ud}$  empirical formula for undrained conditions (constant default value along the pile, initially proposed by Broms [11]). To account for limited soil resistance to close to the ground surface, prEN1997-3:2022 (Annex C.12.2(4)) suggests that  $p_{fd}$  be determined using the following equation:

$$p_{f,d} = c_{ud} \cdot \left(2 + \frac{2}{3} \cdot \frac{z}{D}\right) + \sigma'_z \quad (2)$$

where,  $\sigma'_z$  is the effective vertical stress of the soil at depth  $z$  below the ground surface. Both “2” and “2/3” inside Equation 2 are dimensionless empirical constants (these are discussed later). The subscript “ $d$ ” just denotes design value in Eurocode’s limit state framework. For soft clays, API [3] suggests Matlock’s [17] equation (please compare with Equation 2):

$$p_f = c_u \cdot \left( 3 + J \cdot \frac{z}{D} \right) + \sigma'_z \quad (3)$$

where,  $J$  ranges from 0.25 to 0.5 having been determined by field tests. Actually, Matlock performed field tests at two onshore sites. The value of  $J=0.5$  value correspond to the “Sabine” tests, while the  $J=0.25$  value to the “Lake Austin” tests, although Matlock recommends the use of the 0.5 value in design [22]. Surprisingly, Matlock suggested the least conservative value between the two.

For stiff clays, API [3] does not give a specific formula. However, it prompts to the Reese et al.’s [18] method for the construction of  $p - y$  curves, while mentioning that the ultimate bearing capacity of soil varies between  $8c_u$  and  $12c_u$ . For the history, Reese et al.’s [18] formula is:

$$p_f = \left[ c_u \cdot \left( 2 + 2.83 \cdot \frac{z}{D} \right) + \sigma'_z \right] D \quad (4)$$

At this point it is interesting to mention what each term in Equations 2 to 4 represent and how their general form has been derived. In this respect, the term  $c_u \cdot \left( a + J \cdot \frac{z}{D} \right)$  represents the contribution of soil strength to pile capacity, and the  $\sigma'_z$  term represents the contribution of soil weight to lateral bearing capacity before a localized “flow” around mechanism is formed [13, 17, 18, 23]. The variation of the ultimate soil resistance with depth is based on the “wedge-type-failure theory” and the “flow-around failure theory”, which were both presented by Reese [24]. In their studies, Matlock [17] and Reese et al. [18] assumed a rigid pile translated horizontally, so as to cause the passive failure of a rigid (Coulomb-type) soil wedge in front of the pile; the active state has arbitrarily been neglected behind the pile (this is a major assumption, on the unsafe side). We shall recall that, although these methods are intended for the analysis of long, slender piles, their derivation is based on the consideration of a rigid pile. At great depths (that is, below the lower point of the passive wedge), failure will occur by “flow” of the soil around the pile without vertical displacement. And a question logically arises: In a no-

volume-change deformation under undrained conditions, how the soil can “flow” horizontally? Apparently, this is a major and not valid assumption by both Matlock [17] and Reese et al. [18, 24]. Readers may find useful the freely available U.S. Army Technical Report K-84-2 by Reese et al. [13], where the methodology is explained in detail. It is also important to be mentioned that Equation 4 has been revised by Sullivan, Reese and Fenske [25] to:

$$p_f = \left[ c_u \cdot \left( 2 + 0.833 \cdot \frac{z}{D} \right) + \sigma'_z \right] D \quad (5)$$

For some reason, however, API [3] in 2000 makes reference to the 1975 [18] version instead of the more recent version of 1980 [25], also proposed by Reese.

So far, based on a very limited number of experiments, Matlock [17] and Reese and Fenske [25] suggest that  $J=0.5$  and  $0.833$  respectively, while API [3] and prEN1997-3:2022 standards  $J = 0.25$  to  $0.5$  and  $J = 0.667$  respectively. It may not be coincidence that the  $J = 0.667$  value of prEN1997-3:2022 is the exact average value of  $0.5$  and  $0.833$ . The  $J=2.83$  value in Equation 4, which is much greater than the other values, is the original value derived from Reese et al.’s [13, 18] mathematical analysis (no calibration with field test data). Commenting on the number “3” in Equation 3 and number “2” in Equation 4 (it also appears in Equations 2 and 5), this is a coefficient in front of  $c_u$  for defining the undrained strength of soft and stiff clays at the surface, given by Matlock [17] and Reese et al. [18] respectively. In this respect, someone would expect the coefficient in question to be greater in the case of stiff clays; however, the opposite is observed and probably prEN1997-3:2022 adopted the more conservative value among the two. The readers may have also noticed that Equations 4 and 5 (reproduced as they appear in the original works) contain an extra  $D$  (outside the square brackets). This is the rather rational adjustment of soil resistance to the width of the pile,  $D$ . If neglected here, the width of the pile should be considered in the spring constant [26] for the elemental pile length  $\Delta L$ :

$$K = k \cdot D \cdot \Delta L \quad (6)$$

$K$  has the units of stiffness (e.g., MN/m), whereas  $k = p_f/y_f$  has the units of force per length cubed (e.g., MPa/m or MN/m<sup>3</sup>).

Regarding API’s  $p - y$  method [3] for sands, API sponsored O’Neill and Murchison [19, 20] with the purpose to simplify the original Reese et al.’s [27] procedure without introducing

fundamental changes. In this respect, O'Neill and Murchison [19, 20] suggested a modified  $p - y$  curve just to guarantee a more satisfactory agreement with the full-scale tests performed by Reese and his colleagues [27, 28] at Mustang Island (Texas) [29].

Referring to the original Reese's [27] procedure, this is also based on an assumed passive wedge-type failure of soil in front of a rigid pile (please recall the analysis for clays by Reese et al. [13, 18]). Neglecting the very important fact that a  $p - y$  method for long, flexible piles has erroneously been derived considering a rigid-pile model and a rigid soil wedge in front of the pile, the method developed by Reese et al. [18] was calibrated against specific field test data [27, 28]. Logically thinking, this method may not be suitable for different ground conditions.

For checking the validity of Brinch-Hansen's [21] method for "the ultimate resistance of *rigid* piles against transversal forces" (exact title of publication [21]), we should first recall that this work is for *rigid* and not slender piles. Secondly, this method is intended for rectangular and not circular piles. Thus, so far, the prEN1997-3:2022 standard has violated two of the preconditions of Brinch-Hansen's method. In addition, for better interpreting the validity of his assumptions, it is mentioned that Brinch-Hansen divided the problem into three parts, a) the "pressure at ground surface" (meaning literally at zero depth), where he applied active and passive earth pressures, b) the "pressure at moderate depth" (referring to "reasonably small depths"), where the Rankine's  $45^\circ + \varphi'/2$  passive soil wedge is arbitrarily used with Jaky's [30]  $K_o = 1 - \sin\varphi'$  earth pressure at-rest coefficient and c) the "pressure at great depth", where Brinch-Hansen [31] used the cohesion term with the respective depth factor ( $d_c$ ) of his bearing capacity theory for shallow foundations (published in 1961; for the history, the 1961 theory was revised in 1970 by the same author [32]). For calculating, finally, the pressure at any "arbitrary depth", Brinch-Hansen invented an empirical interpolation function for extracting values between the above cases, while his method has been proposed without validation. Regarding element "c" of the above short list, the author feels that it is not necessary to comment on the appropriateness of the application of a bearing capacity theory for shallow foundations to a laterally loaded pile method. Brinch-Hansen himself does. Brinch-Hansen, in 1970 [32] "tentatively proposed" (use of Brinch-Hansen's words) a new depth factor  $d_c$ , as a replacement of his 1961 [31] version. He also admitted that, for depths greater than one footing



width, it is difficult to calculate the depth factor. In addition to the above, Pantelidis and Christodoulou [8] have shown that the at-rest state share the same soil wedge with the active state; thus, the element “b” mentioned above is also not true.

At this point, we should recall that a laterally loaded pile and an embedded retaining wall are essentially the same problem. The main differences are: a) the pile is solved for its diameter, while the embedded wall is solved per meter length, b) the pile has a concentrated lateral load at the top, which causes the unfavorable condition, while the unfavorable condition in the case of an embedded wall is caused mainly by the earth pressures due to the relative difference in the ground elevation on the two sides of the wall and c) the one dimension (referring to thickness) of the embedded wall is much smaller as compared to the other two dimensions (height and running length), while in the case of piles, the one dimension (meaning the vertical length) is usually much greater than the other two. However, both structures are characterized by their flexural rigidity, where the cross-sectional shape is expressed by the moment of inertia. And a rhetorical question: What is a pile-wall, an embedded wall, or a series of piles in contact, the one after the other? As in the case of embedded walls [7], the problem of laterally loaded piles is an earth pressure analysis problem, requiring the knowledge of the earth pressures at any soil state, especially the intermediate ones on the active and the passive “side”. The state of soil at any point along the pile depends on the amount of bending and/or the amount of translational or rotational movement.

Finally, the shortcomings of the beam-on-spring models ( $p - y$  method) are well-known; the author will only use herein the words of the prEN1997-3:2022 standard itself (Annex D.9(3)): “this is a simplification that assimilates the ground to independent springs”, “due to its empirical nature, values of the coefficient of subgrade reaction should always be determined from comparable experience in similar conditions” and “spring stiffness values are very software specific”. According, also, to Murchison and O’Neill [20], who carried out of a comparison study of four methods (proposed by O’Neill and Murchison [19], Scott [33], Reese et al. [3, 27] and Bogard and Matlock [34]) against real pile tests data, errors evidenced with all methods are high, suggesting that further research into fundamental mechanisms of lateral pile-soil interaction is warranted. Bogard and Matlock’s method is a simplification of Reese et al.’s [3, 27] method, replacing some terms of minor significance with constants. Scott’s method

differs from the other methods in the fact that the  $p - y$  relationship is idealized by two straight line segments, with the second line to have slope equal to  $(k \times y)/4$  (the initial segment, with slope defined by the product  $k \times y$ , is similar to the other methods).

Adopting the point of view of O'Neill and Murchison [20] that “further research into the “fundamental mechanisms of lateral pile-soil interaction” is needed, the method proposed below is a completely different and more rational earth-pressure-based approach.

### 3 The Generalized Coefficient of Earth Pressure

The generalized coefficient of earth pressure [6–9] for  $c' - \varphi'$  soils, being at any state between the at-rest and the active or passive failure state, is given by the following equation:

$$K_{XE} = \frac{1-(2\lambda-1)\sin\varphi_m}{1+(2\lambda-1)\sin\varphi_m} - (2\lambda-1) \frac{2c_m}{(1-a_v)(\sigma_v-u)} \tan\left(45^\circ - (2\lambda-1)\frac{\varphi_m}{2}\right) \quad (7)$$

where,  $c_m$  and  $\varphi_m$  are the mobilized shear strength parameters of soil,  $a_v$  is the vertical pseudo-static coefficient,  $u$  is the pore water pressure and  $\sigma_v$  is the vertical total stress.  $\lambda$  is a soil state dependent coefficient being either 0 or 1, while  $X = O, A, P, IA$  or  $IP$  denoting the at-rest, active, passive, intermediate active and intermediate passive state respectively.

The mobilized cohesion of soil,  $c_m$ , is calculated using Equation 8.

$$c_m = c' \frac{\tan\varphi_m}{\tan\varphi'} \quad (8)$$

The mobilized internal friction angle of soil,  $\varphi_m$ , derives from Equation 9.

$$\varphi_m = Re \left( \sin^{-1} \left( -(2\lambda-1) \frac{b_o + \frac{D_o}{C_o \zeta^\lambda} + C_o \zeta^\lambda}{3\alpha_o} \right) \right) \frac{180}{\pi} (^\circ) \quad (9)$$

where,  $\alpha_o = (1 + e_2^2 \tan^2 \varphi')$ ,  $b_o = 1 - (2(2\lambda-1) e_1 e_2 + e_2^2) \tan^2 \varphi'$ ,  $c_o = (e_1^2 + 2(2\lambda-1) e_1 e_2) \tan^2 \varphi'$ ,  $d_o = -e_1^2 \tan^2 \varphi'$ ,  $D_o = b_o^2 - 3\alpha_o c_o$ ,  $D_1 = 2b_o^3 - 9\alpha_o b_o c_o + 27\alpha_o^2 d_o$ ,

$$C_o = \sqrt[3]{\frac{1}{2} \left( D_1 - \sqrt{D_1^2 - 4D_o^3} \right)}, \quad e_1 = (1 - A_o)/B_1, \quad e_2 = (1 + A_o)/[(2\lambda-1)B_1] +$$

247  $2c'/[(1 - a_v)(\sigma_v - u)(2\lambda - 1)B_1 \tan \varphi']$ , and  $\zeta = -\frac{1}{2} + \frac{\sqrt{3}}{2}i$ . The *Re* notation means that  
 248 only the real part of the number is kept; the imaginary part is infinitesimally small, and thus,  
 249 zero.

250 For the active “side” of the problem (any soil state between the state at-rest and the active  
 251 state),  $\lambda = 1$ . Also,

$$252 \quad A_0 = \frac{1 - \sin \varphi'}{1 + \sin \varphi'} \left( 1 - \xi \sin \varphi' + \tan \theta_{eq} \tan \varphi' (2 + \xi (1 - \sin \varphi')) \right) \quad (10)$$

$$253 \quad B_1 = \frac{2c'}{(1 - a_v)(\sigma_v - u)} \tan \left( \frac{\pi}{4} - \frac{\varphi'}{2} \right) \quad (11)$$

254 For the passive “side” of the problem (any soil state between the state at-rest and the passive  
 255 state),  $\lambda = 0$  when  $A_0 \geq 1$  and  $\lambda = 1$  when  $A_0 \leq 1$ . Also,

$$256 \quad A_0 = \left( \frac{1 + \sin \varphi'}{1 - \sin \varphi'} \right)^{\xi_1} \left( 1 + \xi \sin \varphi' + \xi_2 \tan \theta_{eq} \tan \varphi' (2 + \xi (1 + \sin \varphi')) \right) \quad (12)$$

$$257 \quad B_1 = (2\lambda - 1) \frac{2c'}{(1 - a_v)(\sigma_v - u)} \tan \left( \frac{\pi}{4} - \frac{\varphi'}{2} \right) \left( \frac{\tan \left( \frac{\pi}{4} + \frac{\varphi'}{2} \right)}{\tan \left( \frac{\pi}{4} - \frac{\varphi'}{2} \right)} \right)^{\xi_1} \quad (13)$$

258 where,  $\theta_{eq} = \text{atan} \left( \frac{a_H}{1 - a_v} \right)$  in the absence of pore water pressure or  $\theta_{eq} = \text{atan} \left( \frac{a_H}{1 - a_v} \frac{\sigma_v}{\sigma_v - u} \right)$  in  
 259 the presence of pore water pressure, while  $\xi_1 = 1 + \xi$ ,  $\xi_2 = 2/m - 1$  and  $\xi =$   
 260  $(m - 1)/(m + 1) - 1$ .  $m$  is a real positive number (ranging from 1 to  $+\infty$ ) calculated as fol-  
 261 lows:

$$262 \quad m = \left( 1 + \frac{\Delta y}{\Delta y_M} \left( \frac{H}{z} \right)^{1 + \frac{\Delta y}{\Delta y_M}} \right) \left( 1 - \frac{\Delta y}{\Delta y_M} \right)^{-1} \quad (14)$$

263  $\Delta y_M$  is the required horizontal displacement for the development of the active or passive state  
 264 at the mid-height of the retained soil. That is,  $\Delta y_M = \Delta y_{max}(z/H=0.5)$ . For  $0 \leq z/H \leq 0.5$ ,  
 265  $\Delta y_{max}$  is calculated using Equation 15 for smooth (unfavorable case) piles. For  $0.5 \leq z/H \leq$   
 266 1, the value of  $\Delta y_{max}$  is equal to the one corresponding to  $z/H = 0.5$ .  $H$  is generally the height

of the retained soil (in the present paper, it is either the length of the pile  $L$  or the length of the pile measured from the ground surface to the point of virtual fixity, PVT)

$$\Delta y_{max} = \frac{\pi}{4} \frac{(1-\nu^2)}{E} \frac{(1+z/H)^3(1-z/H)}{z/H} H \cdot \Delta K \cdot (1 - a_v)(\sigma_v - u) \quad (15)$$

$\Delta K = K_{OE} - K_{AE}$  or  $K_{PE} - K_{OE}$ , depending on the case examined while  $E$  and  $\nu$  are the elastic modulus and Poisson's ratio of the retained soil.  $\Delta y_{max}$  becomes maximum for  $z/H=0.5$ .

$\Delta y$  is the deflection of the pile at depth  $z$  calculated based on the theory of elastic beams (see Section 6).

The total earth pressure at depth  $z_A$  (or  $z_P$ ) acting perpendicular to a vertical or nearly vertical retaining structure for any soil state  $X$ , therefore, is

$$\sigma_{XE} = K_{XE}(1 - a_v)(\sigma_v - u) + u \quad (16)$$

#### 4 Proposed method for laterally loaded piles

The earth pressures acting on the circumference of a circular pile not subjected to any external horizontal loading is the earth pressures at-rest. When the pile is loaded laterally, the soil state around the pile changes. The change depends both on the location along the pile and the location on its circumference. And while the former is more obvious because it is related to the movement/deformation of the pile (bending, rotation, translation), the latter needs some explanation. The soil at the two circumference points of the pile on the diameter which is parallel to the direction of the lateral loading will be at the (intermediate) active and (intermediate) passive state respectively; the word "intermediate" has been put in brackets because the failure state may have been reached or not. On the other hand, the soil at the two circumference points of the pile on the diameter which is perpendicular to the direction of the lateral loading will be at the state at-rest. Apparently, the earth pressure at any other circumference point of pile will have an intermediate value between the above two cases. Let us assume, now, a random earth

pressure vector, which acts radially on the circular pile making an angle  $\beta$  (in radians) with the direction of the lateral loading (Figure 1) and that the earth pressure coefficient is given by the following expression:

$$K(\beta) = K_O \left( \frac{\beta}{\pi/2} \right) + K_X \left( 1 - \frac{\beta}{\pi/2} \right) = K_X + (K_O - K_X) \left( \frac{\beta}{\pi/2} \right) \quad (17)$$

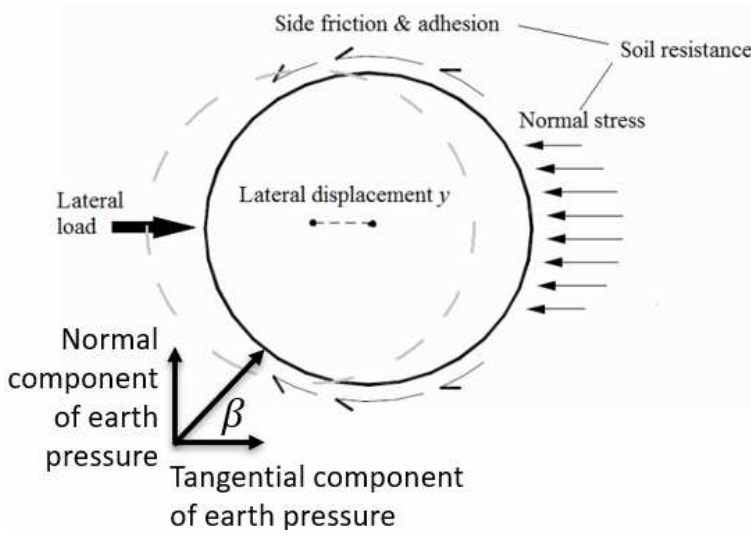


Figure 1. Figure showing the angle  $\beta$  as well as the normal and tangential components of earth pressure.

Studying the earth pressures acting on the pile in the direction parallel to the direction of the lateral load (this direction is called hereinafter “tangential”), the resultant effective force on either active or passive “side” of the pile (per  $dz$  pile length) is:

$$\int_{-\pi/2}^{\pi/2} \left( K_O \left( \frac{\beta}{\pi/2} \right) + K_X \left( 1 - \frac{\beta}{\pi/2} \right) \right) (R \cdot \cos\beta) d\beta (\sigma_V - u) dz = (2R) K_X (\sigma_V - u) dz \quad (18)$$

Applying the principle of superposition between the active and the passive “side” of the pile, the resultant effective “tangential” force at depth  $z$  (per  $dz$  pile length) will be:

$$(2R)(K_{IP} - K_{IA})(\sigma_V - u) dz \quad (19)$$

Calculating, now, the frictional resistance at the pile – soil interface, the resultant effective “normal” force on either left or right side of the pile (with respect to the lateral load) per  $dz$  pile length is:

$$\int_0^\pi \left( K_o \left( \frac{\beta}{\pi/2} \right) + K_x \left( 1 - \frac{\beta}{\pi/2} \right) \right) R d\beta (\sigma_v - u) dz = (\pi R) K_o (\sigma_v - u) dz \quad (20)$$

The rationality of Equation 17 is argued by the very form of Equations 18 and 20.

In practice, however, on the active “side” of the pile the soil becomes loose and thus, the concept of frictional resistance loses its meaning [7]; on the passive “side”, on the other hand, the soil becomes denser, allowing the shearing resistance to be developed on the interface. Thus, the resultant effective normal force on either left or right side of the pile (per  $dz$  pile length), will be the half of the one calculated in Equation 20:

$$\left( \frac{\pi R}{2} \right) K_o (\sigma_v - u) dz \quad (21)$$

Based on the above and considering that two quarter circles of the pile circumference contribute to the frictional resistance (due to symmetry), the total frictional resistance force (per  $dz$  pile length), finally, is:

$$[(\pi R) K_o (\sigma_v - u) \{\tan \varphi'\}_{int}] dz \quad (22)$$

$\{\tan \varphi'\}_{int}$  is the soil-pile interface friction coefficient, with  $\varphi'$  being the peak friction angle of the soil at depth  $z$ . The interface shear resistance, however, is usually taken as a fraction of soil’s shear strength, thus,  $\{\tan \varphi'\}_{int} = \alpha \cdot \tan \varphi'$ , where  $\alpha$  is a shear reduction coefficient (e.g.,  $\alpha = 1, 3/4, 2/3, 1/2$  are rather some commonly used values).

Adhesion is treated in a similar way. Assuming a common reduction coefficient,  $\alpha$ , Equation 22 is extended to its full form:

$$(\pi R) [\{c'\}_{int} + K_o (\sigma_v - u) \{\tan \varphi'\}_{int}] dz = \alpha (\pi R) [c' + K_o (\sigma_v - u) \tan \varphi'] dz \quad (23)$$

Considering Equations 18 and 21, the circular cross-section of the pile could be replaced by an equivalent  $(\pi R / 2) \times 2R$  rectangular one (see Figure 2). This equivalent pile will have a new moment of inertia and a new modulus of elasticity for keeping the same flexural rigidity ( $EI$ ) value of the original problem. The equivalent modulus, moment of inertia and, also, unit weight are:

$$E_{eq} = \frac{12}{\pi^2} E_p \approx 1.22 \cdot E_p \quad (24)$$

$$I_{eq} = \frac{2R (\pi R / 2)^3}{12} = \frac{\pi^3 R^4}{48} = \frac{\pi^2}{12} I_p \approx 0.82 \cdot I_p \quad (25)$$

$$\gamma_{eq} = \gamma_p \frac{\pi R^2}{(2R)(\pi R / 2)} = \gamma_p \quad (26)$$

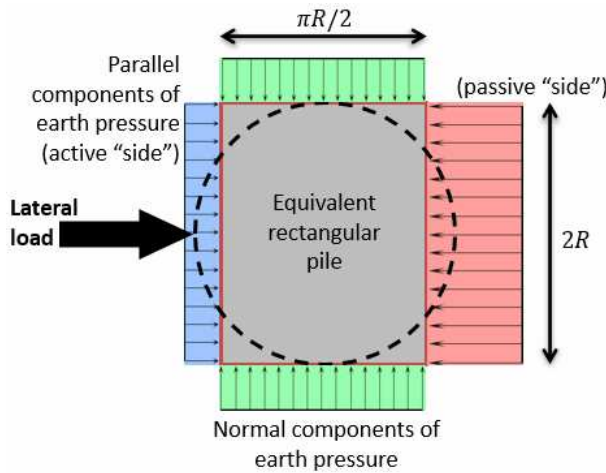


Figure 2. Equivalent  $\pi R / 2 \times 2R$  rectangular pile cross-section with modulus,  $E_{eq} = \frac{12}{\pi^2} E_p$ , moment of inertia,  $I_{eq} = \frac{\pi^2}{12} I_p$ , and unit weight  $\gamma_{eq} = \gamma_p$ .

## 5 Designing for the seismic situation

In the seismic situation with the seismic excitation to act along the direction of the lateral load (unfavorable case), the seismic earth pressure coefficients should be used for the active and passive “side” of the problem. On the contrary, the static earth pressure coefficient should be used for the earth pressure at-rest part of the solution; the static values are also considered for

the mobilized shear strength values of soil for calculating the shearing resistance at the soil – pile interface. Where the calculations involve the unit weight of soil, this becomes  $\gamma(1 \pm \alpha_v)$ . Also, in the framework of a limit state analysis, the lateral load will take the corresponding value.

Regarding the body of the pile itself, a pile inside the ground interrupts the continuity of the latter along the horizontal direction and since its unit weight is greater than the unit weight of the surrounding soil, it acts as inertial mass with different period of vibration,  $T$ . Since  $T$  is proportional to mass (i.e., to unit weight), and the unit weight of (concrete or steel) pile is greater than the unit weight of soil, the pile will be keep moving for a bit longer, while the soil is already returning towards its first full oscillation (and so on). In a pseudo-static analysis, the horizontal stress due to the inertial effect of the pile mass (per  $dz$  pile length) will be:

$$a_h[\gamma_p(\pi R^2)dz]/2R = \left[\frac{\pi}{4}a_h\gamma_p(2R)\right]dz \quad (27)$$

If the pile cross-section is uniform along its length and if there is no spatial variation with depth for the horizontal ground motion, the inertial effect of the pile mass will be constant with depth.

For a seismic excitation acting perpendicularly to the direction of the lateral load, the problem is solved statically.

## **6 Combining the proposed earth pressure theory with static analysis of elastic beams**

An advantage of the proposed method is that piles are not required to be distinguished to “short” or “long” ones. The analysis will show if a laterally loaded pile behaves as “short” or “long”, since not only the bending profile is obtained, but also the amount of translation and/or



rotation (along with the location of the pivot point). The point of virtual fixity of long piles can also be determined, but this is discussed in Section 8. Of course, not only the bending and earth pressure diagrams can be drawn, but also the shear and moment ones. This is of particular importance, in concrete piles, where failure due to the exceedance of shear or moment capacity is possible. The above are feasible because the proposed earth pressure theory is combined the elastic beam theory. Indeed, the proposed method is able to deal with both free-head and fixed-head piles. In this respect, free-head piles are treated as cantilever beams, while fixed-head piles are treated as beams with fixed end in the one end and sliding support in the other end (Figure 3). An elastic beam with point load is used for representing pile with the lateral concentrated load at the top, while an elastic beam with partial trapezoidal load is used for dealing with the earth pressures along the pile (the principle of superposition stands as the pile is divided in a finite number of segments). The required formulae from statics are summarized in the appendix at the end of the paper.

For free- and fixed-head piles the deflection due to the action of a point load is calculated using the following formulae from statics:

$$\Delta y_p(z') = (P - f_{ee}P_{ee}) \frac{(3L-z')z'^2}{6E_p I_p} \quad : \text{ free-head piles} \quad (28)$$

$$\Delta y_p(z) = (P - f_{ee}P_{ee}) \frac{(L-z)^2(L+2z)}{12EI} \quad : \text{ fixed-head piles} \quad (29)$$

$E_p I_p$  is the flexural rigidity of the beam (in this respect, of the pile),  $L$  is the length of the beam (referring to the part of the pile between the point of (virtual) fixity, PVF, and the point of action of  $P$ ) and  $z' = L - z$  ( $z$ -coordinate along the beam measured from its fixed support, i.e., from PVF).  $P_{ee}$  is an equivalent load referring to the strain energy stored in the pile due to bending and subtracted from  $P$  for avoiding the double inclusion of this energy in the proposed

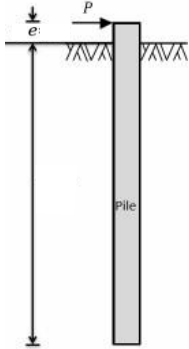
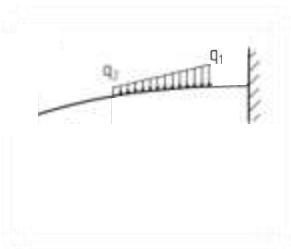
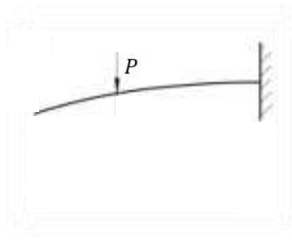
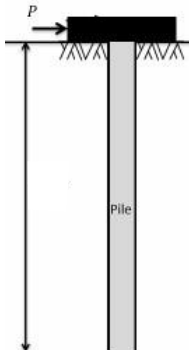
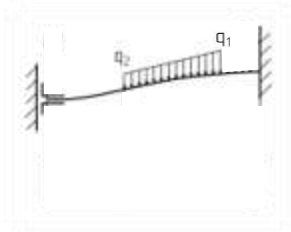
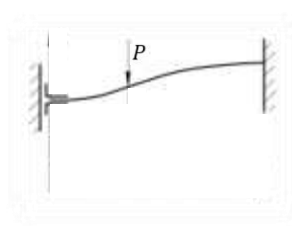
procedure (augmented by a factor  $f_{ee}=1.5$  for calibration purposes against finite elements; this is the only empirical part of the proposed method); it is found using the maximum calculated deflection value,  $\Delta y_{P,max}$  (i.e.,  $P_{ee} = 3\Delta y_{P,max}E_p I_p/L^3$  for free head piles and  $P_{ee} = 12\Delta y_{P,max}E_p I_p/L^3$  for fixed head piles), while an optimization procedure is followed for satisfying two energy criteria (these are discussed later in this paragraph). The deflection values of Equation 28 (or Equation 29) are added to the deflection caused by the earth pressures acting on the two sides of the pile. A number of iterations is needed until convergence, having as starting point the earth pressures at-rest. The general iterative procedure has been described in Pantelidis [7] for the case of embedded retaining walls and thus, it is not repeated here. It is only mentioned that all magnitudes, herein, need to be reduced to the pile diameter (it is reminded that a retaining structure is usually solved per meter length). Also, as in the case of embedded retaining walls, laterally loaded piles, in addition to bending, may be rotated around a pivot point and/or be translated horizontally. In every case, the pile will find its final position satisfying simultaneously: a) the *equilibrium of energy* and b) the *principle of least action*, meaning that, in some sense, the true motion is the optimum out of all possible motions. More specifically, the difference of the *Works Done* by the passive and the active earth pressures must be equal to the strain energy stored in the pile due to bending ( $W_P - W_A = U_{PL}$ ). Also, the total *Work Done* in the two sides must be the least possible.

While the *Work Done* is defined by the product of displacement (deflection at depth  $z$ ) and the respective force, the strain energy  $U$  due to bending [35] is:

$$U_{PL} = \frac{P^2 L^3}{6E_p I_p}; \text{ free-head piles} \quad (30)$$

406  $U_{PL} = \frac{P^2 L^3}{24E_p I_p}$ : fixed-head piles (31)

407 where  $L$  is the distance between the lower end of the pile or the point of (virtual) fixity and the  
 408 point of application of  $P$  (at  $z = 0$  m).

	The problem	Earth pressures	Lateral loading
Free-head "long" pile		Cantilever Beam Under a Distributed Load 	Cantilever Beam Under a Point Load 
Fixed-head "long" pile		Beam with Fixed End and Sliding Support Under a Distributed Load 	Beam with Fixed End and Sliding Support Under a Point Load 

410 *Figure 3. Static analysis of beams: basic cases with application to the problem of laterally loaded piles.*

## 411 7 The case of displacement piles

412 Generally, the procedure described above refers to bored (non-displacement) piles. For dis-  
 413 placement piles, the soil state in the close vicinity of the pile changes during the installation  
 414 face from the state at-rest to an intermediate passive state or, even, to the passive state (Figure  
 415 4a,b). Prior to applying the lateral loading, this soil state will be constituting the new state at-  
 416 rest. Indeed, this change will be directly analogous to the pile radius ( $D/2$ ). More specifically,

the new soil state at any depth (as expressed by the respective earth pressure coefficient,  $K_{IP}$ ) can be found using Equation 15 as follows:

$$\frac{D}{2} = \frac{\pi}{4} \frac{(1-\nu^2)}{E} \frac{(1+z/H)^3(1-z/H)}{z/H} H \cdot (K_{IP} - K_O) \cdot (1 - a_v)(\sigma_v - u) \quad (32)$$

The validity of Equation 15 has been shown in [7, 8]. The coefficient representing the new “overconsolidated state at-rest”, then, is:

$$K_{O,new} = K_{IP} = K_O + \frac{D}{2} \left[ \frac{\pi}{4} \frac{(1-\nu^2)}{E} \frac{(1+z/H)^3(1-z/H)}{z/H} H (1 - a_v)(\sigma_v - u) \right]^{-1} \quad (33)$$

Therefore, the equations in Section 4 have to be modified accordingly, replacing  $K_O$  with  $K_{O,new}$  according to Figure 4b. Apparently, if  $D/2 \geq \Delta x_{max}$ , the earth pressure at the specific depth considered is the passive one.  $K_{O,new}$  can alternatively be expressed with respect to the over-consolidation ratio:

$$K_{O,new} = K_O \left( \frac{K_{O,new}}{K_O} \right) = K_O OCR \quad (34)$$

In the theoretical case that the pile is retracted from the ground, the soil will not rebound to its original position. This irreversible deformation of the soil is accompanied by stress “trapping”. Adopting Mayne and Kulhawy’s [36] correction, the new “overconsolidated state at-rest” coefficient on the active “side” of the problem will be  $K_O(OCR)^{\sin \phi}$  according to Figure 4c. On the other hand, the “trapped” stresses on the passive “side” of the problem remain unfavorable and thus, the  $K_{O,new}$  coefficient should be applied.

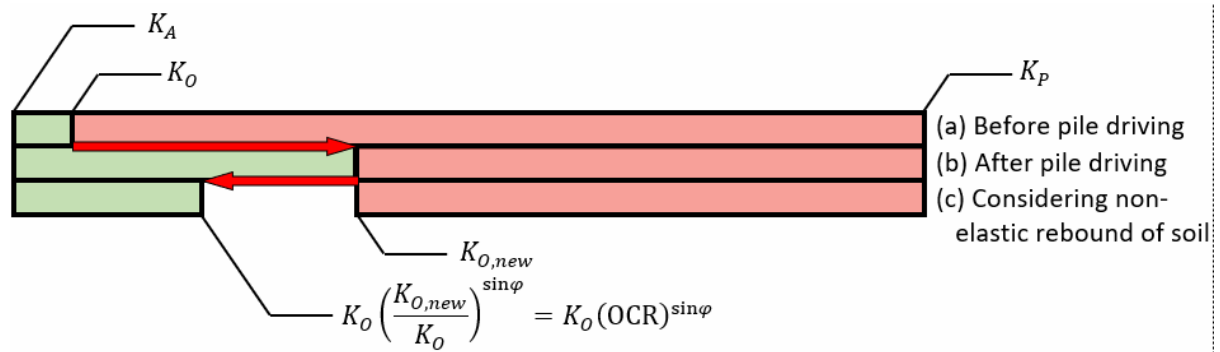


Figure 4. Change in the state at-rest of soil due to pile driving.

An example is given. Let, a 10-meter-long pile of diameter  $D = 2\Delta y$  (various  $\Delta y$  values will be considered) driven into a cohesionless soil with  $\phi' = 30^\circ$  and modulus of elasticity and Poisson's ratio equal to 20,000 kPa and 0.3 respectively. The new state at-rest, as expressed by the respective earth pressure coefficient, for  $\Delta y = 0.05, 0.1, 0.2$  and  $0.3$  m is shown in Figure 5. The black solid lines represent the  $K_{O,new}$  coefficient, standing for the passive "side" of the problem, while the red dashed lines represent the  $K_O(OCR)^{\sin \phi}$  coefficient, standing for the active "side" of the problem (recall Figure 4c). A  $\Delta y = 0.302$  m value is required for the specific soil to reach its passive state (at any depth).

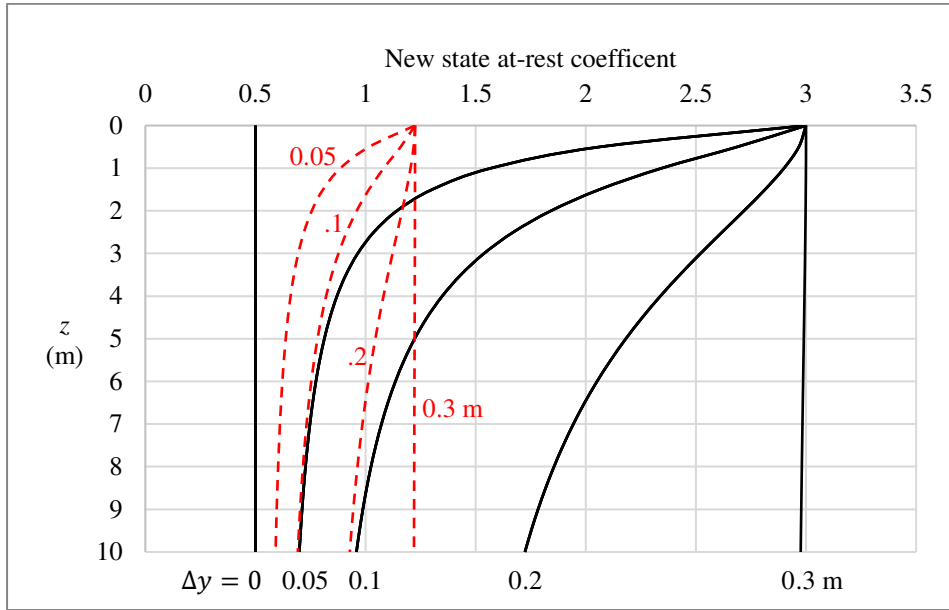


Figure 5. New state at-rest coefficient for considering soil compaction due to pile driving into the ground (example curves). Black solid lines:  $K_{0,new}$  standing for the passive side of the problem. Red dashed lines:  $K_0(OCR)^{\sin\phi}$  standing for the active side of the problem.

## 8 Location of the point of virtual fixity (PVF) of pile

A pile embedded in the soil can be regarded as properly restrained in position and direction at the “point of virtual fixity” in the soil [37]; the point of virtual fixity (PVF) is a zero-deflection point, where the bending moment in the pile becomes maximum and the earth pressures on the two sides of the pile are the earth pressures at-rest, which are equal and opposite. The location of the PVF is found by a trial-and-error procedure, for finding the point above which the pile satisfies the two energy criteria mentioned in Section 6. Below this point the deflection and thus the work done is zero.

## 9 Three-dimensional passive soil wedge in front of the pile

On the passive “side”, normally, a three-dimensional soil wedge resists to the pile movement/deformation; this concept was first introduced by Reese [24], although Reese’s soil wedge was a passive failure wedge (Figure 6).

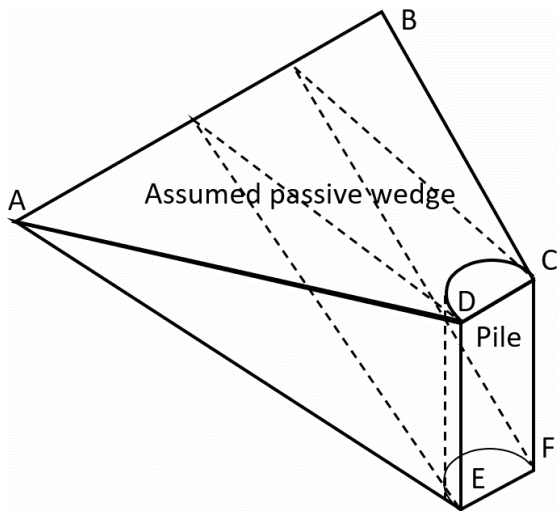


Figure 6. General shape of the assumed passive wedge-type failure according to Reese et al. [27]

In this respect, some observations can be made. The bottom area of this soil wedge (ABFE in Figure 6), which is the main shearing plane of the problem considered, is triangular and thus, larger than the respective rectangular one defined by the width of the pile. As the proposed method considers the second one, it is on the safe side. Second, the soil wedge has two side planes (ADE and BCF in Figure 6), which also play the role of shearing planes in the various  $p - y$  methods (e.g., [13, 17, 18, 23, 24]). The (favorable) effect of these two planes, however, is ignored in the present method; rationally thinking, as the soil wedge moves or tend to move away from its original position to a direction that does not favor contact, no shearing resistance is developed.

The formation of a three-dimensional wedge can be taken into account in the present method simply considering a) an augmenting coefficient to the unit weight of soil related to the greater

volume of the passive soil wedge and b) an augmenting coefficient to the cohesion of soil related to the greater surface area of the base of passive soil wedge. This has been left for future work.

## 10 Application example

The examples presented herein has been solved both with the proposed analytical method (using KPILE v.1 educational software programmed by Dr Panagiotis Christodoulou and the author) and with Rocscience's RS2. Apparently, a laterally loaded pile is a three-dimensional problem. However, ignoring (at least for the moment) the lateral frictional resistance (assumption of perfectly smooth pile) and the fact that a three-dimensional soil wedge is actually affected in front of the pile (passive "side"), the problem is reduced to a plane-strain problem.

A complete analysis requires the pile to be free to bend, translate horizontally and rotate around a pivot point (the latter usually lies somewhere at its lower half). And this because the pile wants to find its final position satisfying the two energy criteria mentioned previously. This optimization involves (in addition to bending) the determination of the horizontal displacement, the angle of rotation and the pivot point. Allowing the *principle of least action* (second criterion) to be violated for the sake of simplicity (e.g., pile free to bend and translate horizontally), a solution that satisfies the *equilibrium of energy* (first criterion) can still be found, however this will not be the optimal one. The same conditions can easily be applied to finite element analysis for direct comparison.

In the example presented below the pile is 12-meters long, although in the finite element analysis the pile was made 20-meters in length to ensure fixity or sliding fixity at depth  $z = 12$  m (that is, the same horizontal displacement is given from  $z = 12$  m to  $z = 15$  m). The geometry,



mesh and boundary conditions are shown in Figure 7. The pile is free to bend from  $z = 0$  to 12 m under the influence of a  $P = 200$  kN horizontal load. The latter is applied at the ground level ( $z = 0$  m) in 11 steps with 20 kN interval. The pile, which is solid and of circular cross-section (with one meter diameter, modulus of elasticity  $E_p = 30$  GPa and thus, flexural rigidity  $E_p I_p = 1.472.622$  KPa  $\cdot$  m<sup>4</sup>), functions in a homogenous, isotropic mass with cohesion  $c' = 0$  kPa, internal friction angle  $\varphi' = 35^\circ$ , unit weight  $\gamma = 16$  kN/m<sup>3</sup>, Young's modulus  $E = 20$  MPa and Poisson's ratio  $\nu = 0.3$ . Pore-water pressures and seismic excitation was ignored for the sake of simplicity. Favoring reproduction of the example problem, all relevant information is given below (if something is not mentioned, the RS2 default value was used). The “*Gaussian elimination*” solver type was used. Regarding the “*stress analysis*” menu, the maximum number of iterations was 1000, the tolerance was set to 0.001, while the “*comprehensive*” convergence type was adopted. The “*mesh type*” was set to “*graded*”, while 6-noded triangular elements were used (meaning 19.0 nodes/m<sup>2</sup> or 9.2 elements/m<sup>2</sup>; see Figure 7). The “*field stress type*” was “*gravity*” with “*stress ratio*” in- and out-of-plane equal to 0.4264 (use of Equation 1 for zero displacement and static conditions). The “*initial element loading*” was “*field stress and body force*”. The problem was solved statically ( $a_h = a_v = 0$ ). The soil parameters were those given earlier (apparently, the “*plastic*” material type was chosen). The pile was modeled as “*structural interface*”, with a “*standard beam*” element as liner and a “*joint*” element at both sides. The liner was considered to be “*elastic*” with Young's modulus  $E_p = 30$  GPa and thickness 0.8383 m; this combination of values gives the same flexural rigidity  $E_p I_p$  as in the analytical solution. The Poisson's ratio of the liner was 0.3, while the “*Timoshenko*” beam element formulation was adopted. Regarding “*joint*”, the “*material dependent*” slip criterion was chosen with zero “*interface coefficient*” (besides, the proposed earth pressure analysis method is for

smooth structures). Both the normal and shear stiffness of the joint element was set to 200 MPa/m.

Regarding the proposed analytical procedure, the deflection  $\Delta y$  (at any depth  $z$ ) is calculated combining the proposed earth pressure method with the elastic beam theory, where the pile is treated as a cantilever beam; the earth pressures on the two sides of the pile along with the lateral loading  $P$  constitute the loading acting on the beam. An iterative procedure is needed. As a starting point (1st iteration), it is logical and convenient to assume that the soil on both sides of the pile is at the state at-rest. However, since a horizontal load acts, this state will change; the pile will have the tendency to bend towards the passive “side”. The deflection ( $\Delta y_{tot}$ ) of the pile caused by the combined action of the earth pressures on the two sides of the pile and the horizontal load is then calculated. For the 2nd iteration these  $\Delta y_{tot}$  values are the new  $\Delta y$  data values for calculating the updated earth pressure coefficients and so on, until convergence to be achieved. This is first done for zero horizontal displacement. If the *equilibrium of energy* is not satisfied, the same procedure is repeated for various displacement values until its satisfaction. For the problem considered here, a horizontal displacement 10.121 mm of the pile was necessary.

The results obtained in the 10<sup>th</sup> iteration are compared against the respective numerical ones in Figures 8 and 9 (deflection and earth pressure charts against depth). The maximum deflection value (at the top of the pile) against the number of iterations is shown in Figure 10, indicating that the problem was already adequately stable in the 5<sup>th</sup> iteration. The earth pressure coefficient values against depth for both sides of the pile have been drawn in Figure 11. More specifically, Figure 8 shows an excellent prediction for the deflection of the pile. Indeed, an active state failure zone exists at the first three meters. Figure 9 shows very good agreement for the

earth pressures on the active “side” (the earth pressure on the passive “side” obtained by the finite element analysis appear to be everywhere bloated and especially near the top).

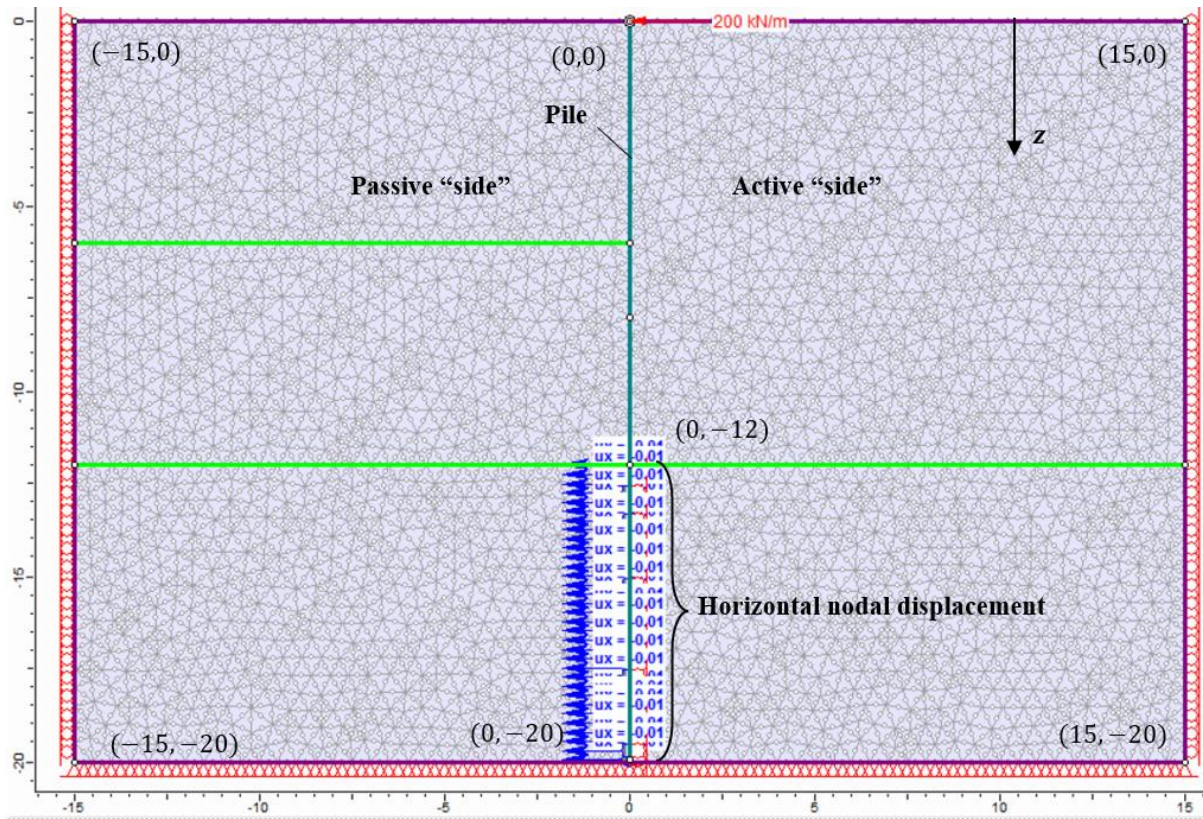


Figure 7. Geometry, mesh and boundary conditions of the RS2 model.

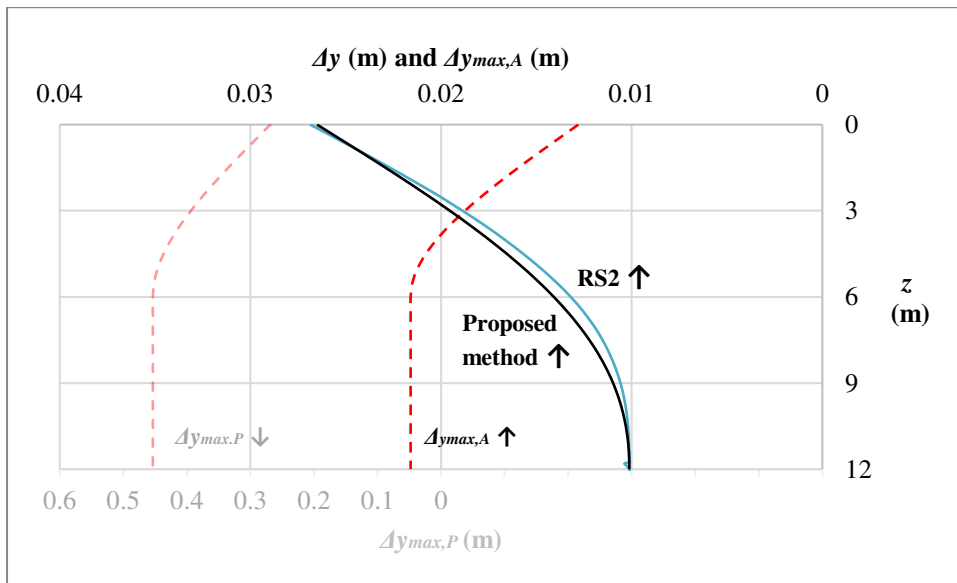


Figure 8. Deflection of pile versus depth chart. Note:  $\Delta y_{\max,P} / \Delta y_{\max,A} = 20.998$ .

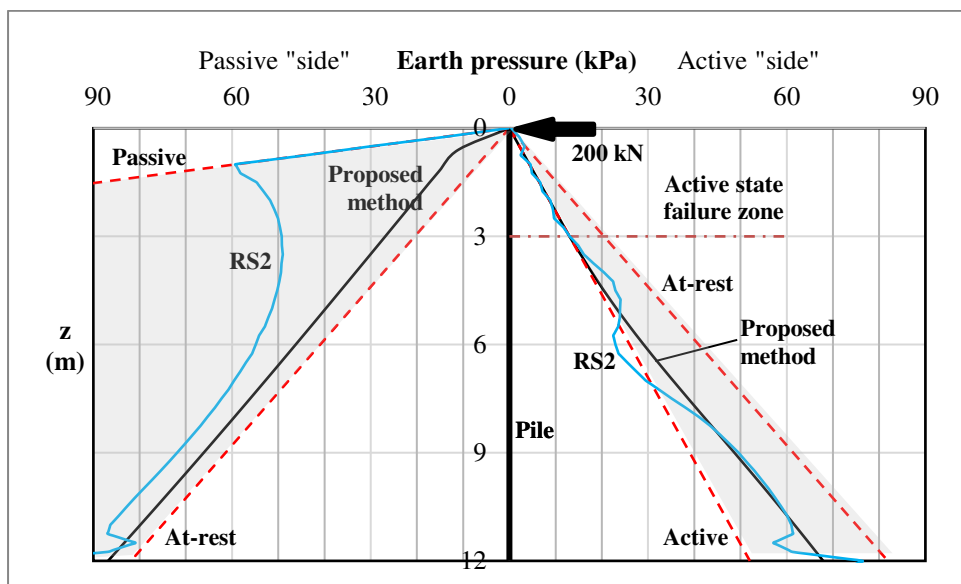


Figure 9. Earth pressures versus depth chart. The red dashed lines indicate the “active”, “passive” and “at-rest” state. Shaded areas indicate the allowable earth pressure values.

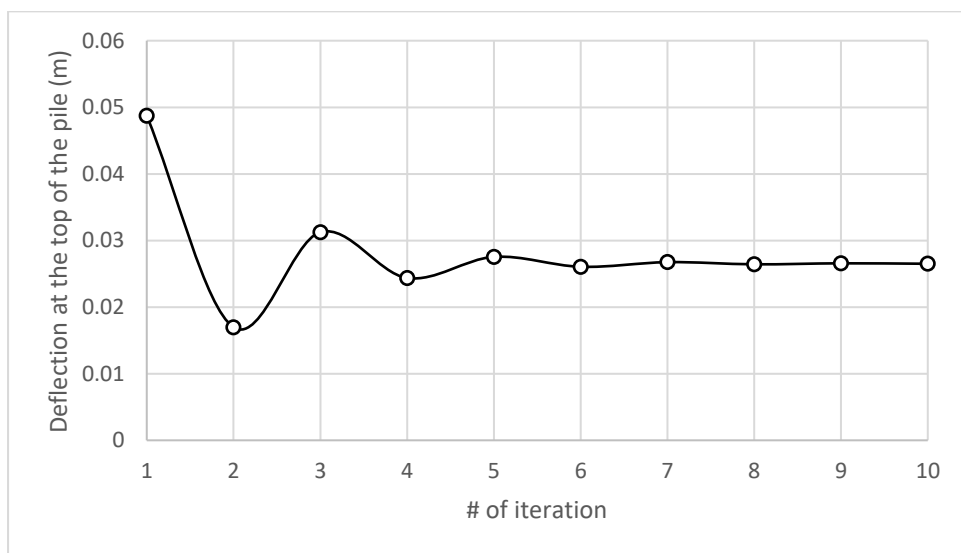


Figure 10. Deflection at the top of the pile versus number of iteration chart.

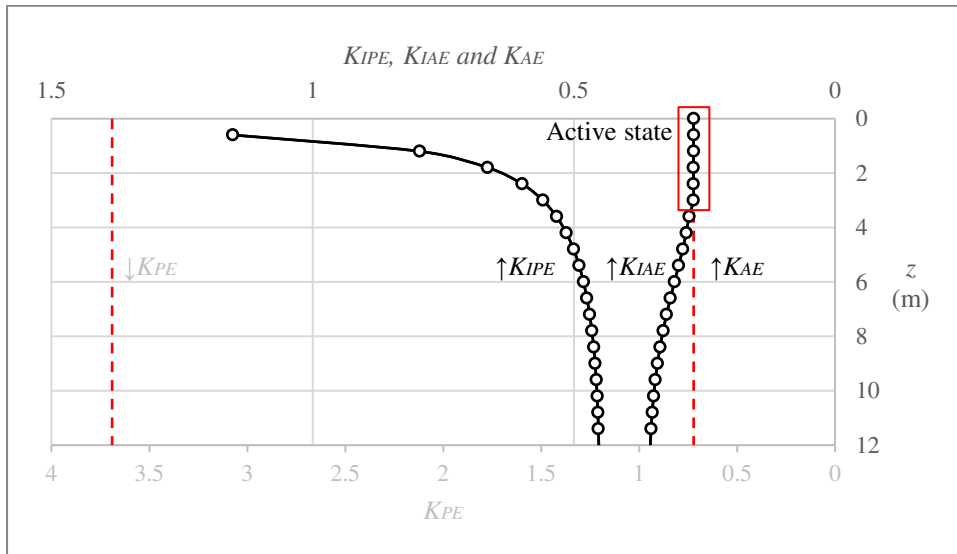


Figure 11. Earth pressure coefficients versus depth chart.

Now the question is, if in the above problem the pile was much longer, so that to behave as long pile which floats in a soil medium, would the deformation pattern obtained by the analytical solution be similar to the numerical one? And what happens to the earth pressures on the two sides of the pile?

Working with the proposed analytical method, the pile was extended up to the length where the two energy criteria were satisfied and found that the “point of virtual fixity” lies at depth 12.66 m from the ground surface. Let say now that the total pile length is 19.95 m, meaning that, for  $12.66 \text{ m} \leq z \leq 19.95 \text{ m}$  the pile keeps its original position prior to loading. The above problem was solved again but this time numerically, giving to the pile the freedom to bend, translate and rotate (pile floating into the ground without any movement restriction).

The results are shown in Figures 12 to 15. From Figure 12 it is clear that the proposed analytical method effectively predicted the deformed shape of the pile, although the numerical point of virtual fixity was found to be slightly lower. Very good agreement was also found in the earth pressures acting on the active “side” of the pile (Figure 13). As for the earth pressures

on the passive “side” of the problem, the numerical model, similarly to the previous example, bloated results.

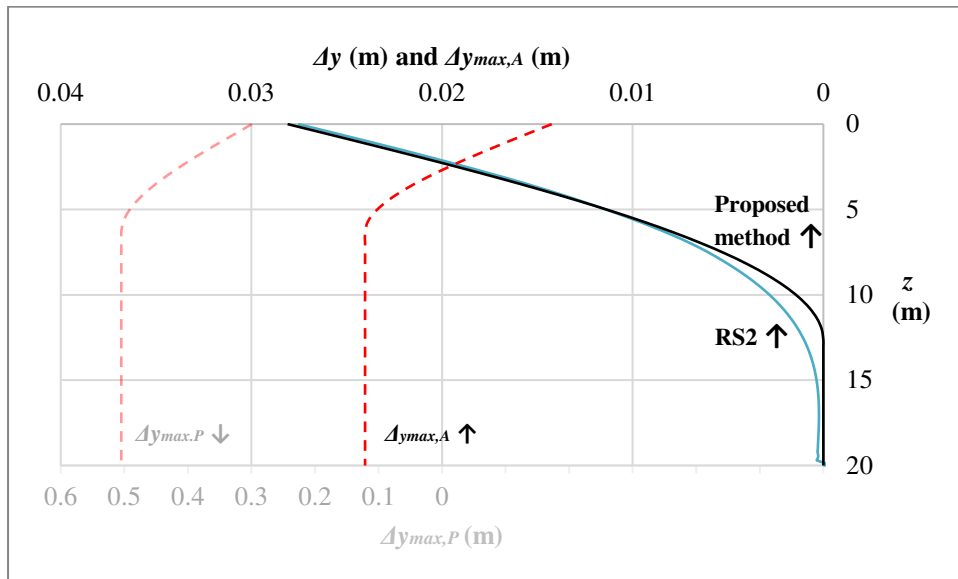


Figure 12. Deflection of pile versus depth chart. Note:  $\Delta y_{max,P} / \Delta y_{max,A} = 20.998$ .

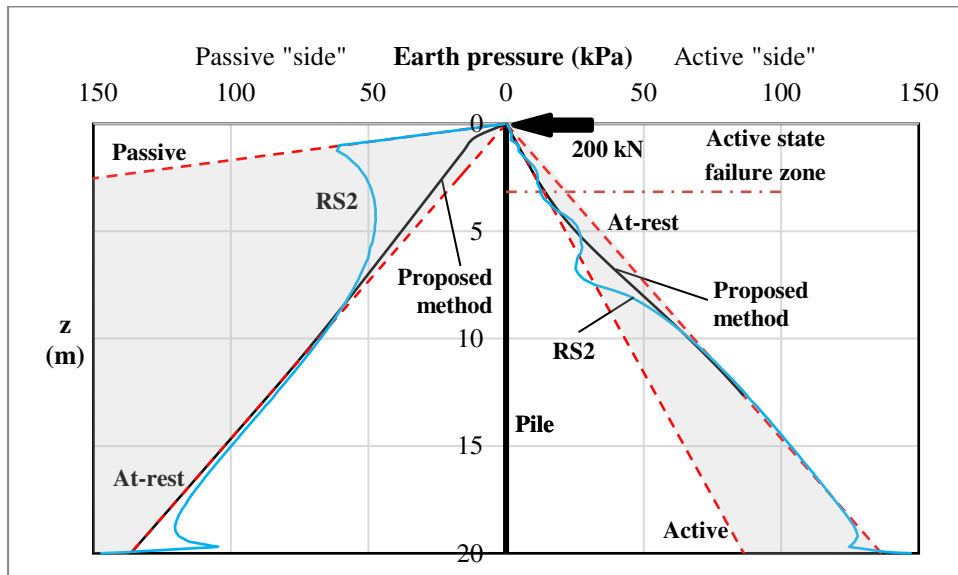


Figure 13. Earth pressures versus depth chart. The red dashed lines indicate the “active”, “passive” and “at-rest” state. Shaded areas indicate the allowable earth pressure values.

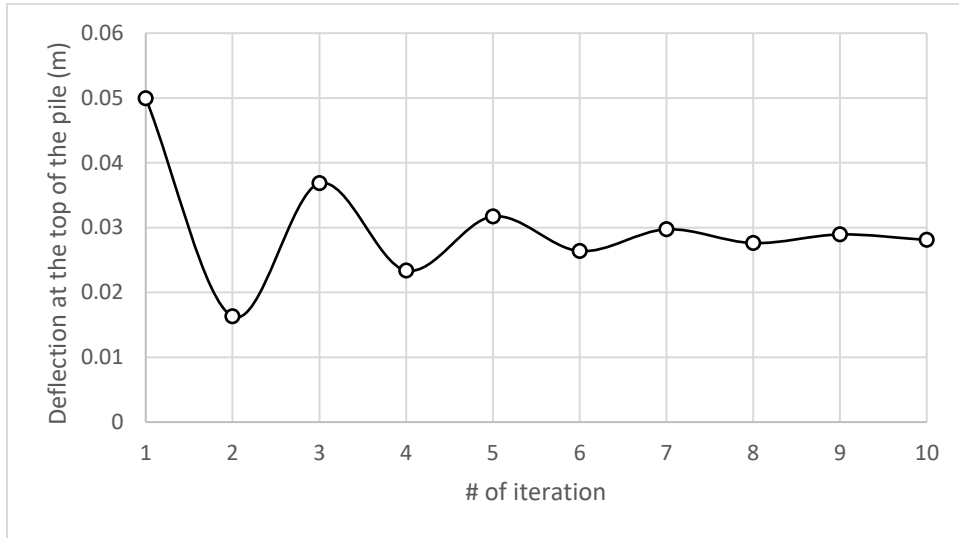


Figure 14. Deflection at the top of the pile versus number of iteration chart.

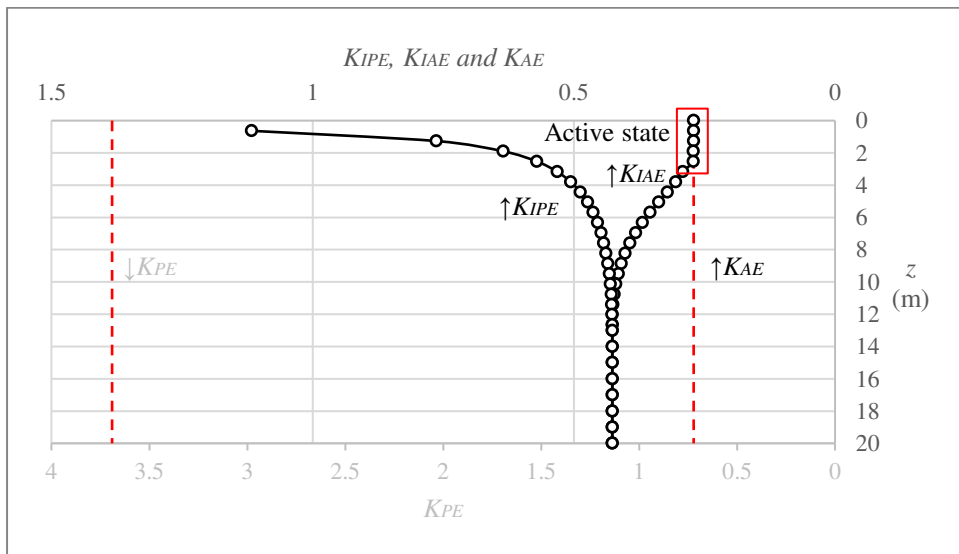


Figure 15. Earth pressure coefficients versus depth chart.

## 11 Conclusions

The problem of a laterally loaded pile is an earth pressure analysis problem, demanding the knowledge of earth pressures of any state between the at-rest and the active or the passive state. However, in the absence of a reliable method for the calculation of the intermediate earth pressures, the current design standards rely on the  $p - y$  method, where the soil is replaced by an

array of parallel springs. The literature review carried out by the author revealed several serious weaknesses of the various  $p - y$  methods, raising queries about their reliability, as well as their validity beyond the very limited field test cases having been used for their calibration.

On the other hand, in 2019 the author proposed a continuum mechanics approach for deriving earth pressure coefficients for any soil state between the at-rest state and the active or the passive state, applicable to cohesive-frictional soils and both horizontal and vertical pseudostatic conditions. An analytical expression for the calculation of the required structure movement for the mobilization of the active or passive failure state of soil is also provided. The proposed method combines these expressions with the static analysis of elastic beams, offering complete earth pressure and pile deflection diagrams, the inertial effect of a possible seismic event (in a pseudostatic manner), as well as the overconsolidation caused by a displacement pile to the surrounding soil. Finally, the location of the point of virtual fixity, which is an important parameter in the case of long, slender piles, is calculated following the proposed procedure.

Adopting the point of view that further research into the fundamental mechanisms of lateral pile-soil interaction is needed, the method proposed herein is a completely different and more rational, earth-pressure-based approach. Indeed, the same approach has been successfully applied by the author to embedded retaining walls, which is a plane-strain problem. The material presented herein was an introduction of the proposed method. Since the problem of a laterally loaded pile is a three-dimensional problem, future work will be focused on the validation and (if necessary) the calibration of the proposed method against three-dimensional finite element analysis and field test data.

## Appendix

- Cantilever beam with point load (Figure 3b)

$$\text{Shear force at } z: V(z) = \begin{cases} P, & 0 \leq z' \leq a \\ 0, & a \leq z' \leq L \end{cases}$$



612 Bending moment at  $z$ :  $M(z) = \begin{cases} -P(a - z'), & 0 \leq z' \leq a \\ 0, & a \leq z' \leq L \end{cases}$

613 Deflection at  $z$ :  $\Delta y(z) = \begin{cases} \frac{Pz'^2(3L-z')}{6EI_P}, & 0 \leq z' \leq a \\ \frac{Pa^2(3L-a)}{6EI_P}, & a \leq z' \leq L \end{cases}$

614 - Cantilever beam with partially distributed trapezoidal load (Figure 3a)

615 Shear force at  $z$ :  $V(z) = \begin{cases} R_A, & 0 \leq z' \leq a \\ R_A - \frac{q_1+q_2}{2}z_a, & a < z' < L - b \\ 0, & z' \geq L - b \end{cases}$

616 Bending moment at  $z$ :  $M(z) = \begin{cases} R_A z' + M_A, & 0 \leq z' \leq a \\ R_A z' + M_A - \frac{2q_1+q_2}{6}z_a^2, & a < z' < L - b \\ 0, & z' \geq L - b \end{cases}$

617 Deflection at  $z$ :  $\Delta y(z) = \begin{cases} -\frac{R_A z'^3}{6EI_P} - \frac{M_A z'^2}{2EI_P}, & 0 \leq z' \leq a \\ -\frac{R_A z'^3}{6EI_P} - \frac{M_A z'^2}{2EI_P} + \frac{4q_1+q_2}{120EI_P}z_a^4, & a < z' < L - b \\ -\frac{R_A L_b^3}{6EI_P} - \frac{M_A L_b^2}{2EI_P} + \frac{4q_1+q_2}{120EI_P}L_q^4 - \theta_B(z' - L_b), & z' \geq L - b \end{cases}$

618 Reactions at the fixed support:  $R_A = L_q q_m, M_A = -\frac{3a+L_q}{3}L_q q_m - \frac{L_q^2}{6}q_2$

619 Also,  $z_a = z' - a, L_q = L - a - b, L_1 = L + a - b, L_b = L - b, q_m = (q_1 + q_2)/2,$

620  $q_z = q_1 + (q_2 - q_1)z_a/L_q, \theta_B = -L_q \frac{(2a^2+L_1^2)q_m+L_1L_qq_2}{12EI_P}$

621 - Beam with fixed end and sliding support under a point load (Figure 3d)

622 Shear force at  $z$ :  $V(z) = \begin{cases} 0, & 0 \leq z \leq a \\ P, & a \leq z \leq L \end{cases}$

623 Bending moment at  $z$ :  $M(z) = \begin{cases} -P\frac{(L-a)^2}{2L}, & 0 \leq z \leq a \\ P\left(z - \frac{L^2+a^2}{2L}\right), & a \leq z \leq L \end{cases}$

624 Deflection at  $z$ :  $\Delta y(z) = \begin{cases} \frac{P(L-a)^2(L^2+2aL-3z^2)}{12E_P I_P}, & 0 \leq z \leq a \\ \frac{P(L-z)^2(L^2+2Lz-3a^2)}{12E_P I_P}, & a \leq z \leq L \end{cases}$

625 - Beam with fixed end and sliding support with partially distributed trapezoidal load (Fig-  
626 ure 3c)

627 Because the expressions are lengthy, it is more convenient, without sacrificing accu-  
628 racy, the beam (pile) to be divided in very small segments of length  $\Delta z$  and treating the  
629 trapezoidal load as equivalent point load,  $P_{eq} = \frac{q_1+q_2}{2} \Delta z$ .

630 Note: In the equations above,  $L$  is the total length of the beam (pile);  $z' = L - z$  is measured  
631 from the fixed support (applicable to cantilever beams), while  $z$  is measured from the sliding  
632 support (applicable to beams with fixed end and sliding support at the two ends).

### 633 **Notation**

634  $\alpha$  = a shear reduction coefficient

635  $a_h$  = the seismic coefficient of horizontal acceleration

636  $a_v$  = the seismic coefficient of vertical acceleration (if negative, the vertical pseudo-static force  
637 acts downwards, i.e., it increases the unit weight of soil,  $(1 + a_v)\gamma$ )

638  $\beta$  = the angle formed by any random earth pressure vector, which acts radially on the circular  
639 pile and the direction of the lateral loading

640  $\gamma$  = the unit weight of soil

641  $\gamma_{eq}$  = the equivalent unit weight of the pile

642  $\gamma_p$  = the unit weight of the pile

643  $\Delta K = K_{OE} - K_{AE}$  or  $K_{PE} - K_{OE}$

644  $\Delta y$  = the wall displacement

645  $\Delta y_{max}$  = the lateral displacement of wall corresponding to the active or passive state; the sym-  
 646 bols  $\Delta y_{max,A}$  and  $\Delta y_{max,P}$  are also used for the active and passive state respectively

647  $\Delta y_M$  = the required horizontal displacement for the development of the active or passive state

648  $\Delta y_{tot}$  = the deflection of the pile caused by the combined action of the earth pressures on the  
 649 two sides of the pile and the horizontal load at the mid-height of the retained soil

650  $\theta_{eq} = \text{atan}\left(\frac{a_h}{1-a_v}\right)$  in the absence of pore water pressure or  $\text{atan}\left(\frac{a_h}{1-a_v} \frac{\sigma_v}{\sigma_v-u}\right)$  in the presence of  
 651 pore water pressure

652  $\lambda$  = a soil state dependent coefficient being either 0 or 1

653  $\nu$  = the Poisson's ratio of the retained soil

654  $\xi = (m - 1)/(m + 1) - 1$ .

655  $\xi_1 = 1 + \xi$  (parameter related to the transition from the soil wedge of the state at-rest to the  
 656 soil wedge of the passive state)

657  $\xi_2 = 2/m - 1$  (same as  $\xi_1$ )

658  $\sigma'_z$  = the effective vertical stress of the soil at depth  $z$  below the ground surface

659  $\sigma_v$  = the vertical total stress

660  $\varphi'$  = the effective internal friction angle of soil

661  $\varphi_m$  = the mobilized friction angle of soil

662  $c'$  = the effective cohesion of soil

663  $c_m$  = the mobilized cohesion of soil

664  $c_{ud}$  = the undrained shear strength of soil (design value)

665  $c_u$  = the undrained shear strength of soil

- 666  $\{c'\}_{int}$  = the soil-pile interface adhesion
- 667  $D$  = the diameter of pile
- 668  $d_c$  = depth factor
- 669  $E$  = the elastic modulus of the retained soil
- 670  $E_{eq}$  = the equivalent modulus of the pile
- 671  $E_p$  = Young's modulus of the pile
- 672  $f_{ee}$  = calibration factor
- 673  $H$  = the height of the retained soil (in the present paper, it is either the length of the pile  $L$  or
- 674 the length of the pile measured from the ground surface to the point of virtual fixity, PVT)
- 675  $I_p$  = moment of inertia of the pile
- 676  $I_{eq}$  = the equivalent moment of inertia of the pile
- 677  $J$  = empirical factor
- 678  $K_o$  = Jaky's (static) coefficient of earth pressure at-rest
- 679  $K_{AE}$ ,  $K_{PE}$  or  $K_{OE}$  = the active, passive or at-rest coefficients of earth pressure in the seismic
- 680 situation (without "E" denote static conditions)
- 681  $K$  = the spring constant (it has the units of stiffness e.g., MN/m)
- 682  $k$  = the horizontal modulus of subgrade reaction of soil ( $k = p_f/y_f$  has the units of force per
- 683 length)
- 684  $K_{XE}$  = the earth pressure coefficient of soil state X ( $X = O, A, P, IA$  or  $IP$  denoting the at-rest,
- 685 active, passive, intermediate active and intermediate passive state respectively)
- 686  $L$  = length of pile
- 687  $m$  = real positive number ranging from 1 to  $+\infty$

688 OCR = overconsolidation ratio

689  $p_f$  = the lateral pressure of the ground at failure

690  $p$  = the lateral pressure

691  $P_{ee}$  = an equivalent load referring to the strain energy stored in the pile

692  $R$  = the radius of the pile

693  $\{\tan\varphi'\}_{int}$  = the soil-pile interface friction coefficient

694  $u$  = the pore water pressure

695  $y_f$  = the transversal deflection of the pile

696  $z$  = the depth  $z$  below the ground surface ( $z_A$  and  $z_P$  refer to the depth on the active and the  
697 passive side respectively)

698  $z' = L - z$  ( $z$ -coordinate along the beam measured from its fixed support, i.e., from PVF)

## 699 **Data availability statement**

700 All data generated or used during the study are available from the corresponding author by  
701 request.

## 702 **Declaration of Competing Interest**

703 The author declare that they have no known competing financial interests or personal rela-  
704 tionships that could have appeared to influence the work reported in this paper.

## 705 **References**

- 706 1. EN1997-1 (2004) Eurocode 7: Geotechnical design, Part 1: General rules. European  
707 Committee for Standardization, Brussels
- 708 2. prEN1997-3:2022 (2022) Eurocode 7 - Geotechnical design - Part 3: Geotechnical  
709 structures (draft standard)

- 710 3. API (2000) Recommended Practice 2A-WSD. Planning, Designing, and Constructing  
711 Fixed Offshore - Working Stress Design (21st edition; including errata and supplement  
712 un to 3, August 2007). Washington
- 713 4. Hannigan PJ, Rausche F, Likins GE, et al (2016) Geotechnical Engineering Circular No.  
714 12–Volume I Design and Construction of Driven Pile Foundations
- 715 5. AASHTO (American Association of State Highway and Transportation Officials)  
716 (2010) LRFD Bridge Design Specifications, 5th ed. Washington, DC
- 717 6. Pantelidis L (2019) The Generalized Coefficients of Earth Pressure: A Unified  
718 Approach. Appl Sci 9:5291
- 719 7. Pantelidis L (2022) Designing embedded retaining walls relying on the Generalized  
720 Coefficient of Earth Pressure and the elastic beam theory. ResearchSquare (preprint):  
721 <https://doi.org/10.21203/rs.3.rs-2132476/v2>
- 722 8. Pantelidis L, Christodoulou P (2022) Comparing Eurocode 8-5 and AASHTO methods  
723 for earth pressure analysis against centrifuge tests, finite elements, and the Generalized  
724 Coefficients of Earth Pressure. ResearchSquare (preprint):  
725 <https://doi.org/10.21203/rs.3.rs-1808466/v3>
- 726 9. Pantelidis L (2022) Shaft resistance capacity of axially loaded piles in cohesive-  
727 frictional soils under static or pseudo-static conditions based on ground parameters.  
728 ResearchSquare (preprint): <https://doi.org/10.21203/rs.3.rs-1986330/v1>
- 729 10. Hannigan PJ, Rausche F, Likins GE, et al (2016) Geotechnical Engineering Circular No.  
730 12–Volume I Design and Construction of Driven Pile Foundations
- 731 11. Broms BB (1964) Lateral resistance of piles in cohesive soils. J soil Mech Found Div  
732 90:27–63
- 733 12. Reese LC (1984) Handbook on design of piles and drilled shafts under lateral load
- 734 13. Reese LC, Cooley LA, Radhakrishnan N (1984) Laterally Loaded Piles and Computer  
735 Program COM624G.
- 736 14. Russo G (2016) A method to compute the non-linear behaviour of piles under horizontal  
737 loading. Soils Found 56:33–43. <https://doi.org/10.1016/j.sandf.2016.01.003>
- 738 15. Russo G, Viggiani C (2008) Piles under horizontal load: an overview. In: Foundations:  
739 proceedings of the second British Geotechnical Association International Conference on

- Foundations, ICOF. pp 24–27
16. European\_Commission (2015) English Style Guide. A Handbook for Authors and Translators in the European Commission (updated Sept. 2022)
  17. Matlock H (1970) Correlation for design of laterally loaded piles in soft clay. In: Offshore technology conference. OnePetro
  18. Reese LC, Cox WR, Koop FD (1975) Field testing and analysis of laterally loaded piles on stiff clay. In: Offshore technology conference. OnePetro
  19. O'Neill MW, Murchison JM (1983) An evaluation of p-y relationships in sands. Research Rep. No. GT-DF02-83. University of Houston, Houston
  20. Murchison JM, O'Neill MW (1984) Evaluation of p-y relationships in cohesionless soils. In: Analysis and design of pile foundations. ASCE, pp 174–191
  21. Brinch-Hansen J (1961) The ultimate resistance of rigid piles against transversal forces. Geotek Instit, Bull
  22. Meyer BJ, Reese LC (1979) Analysis of single piles under lateral loading. Center for Highway Research, University of Texas at Austin TX
  23. Zhang Y, Andersen KH, Tedesco G (2016) Ultimate bearing capacity of laterally loaded piles in clay—Some practical considerations. Mar Struct 50:260–275
  24. C. RL (1958) Discussion of “Soil Modulus for Laterally Loaded Piles,” by Bramlette McClelland and John A. Focht, Jr. (ASCE Proceedings Paper 1081). Transactions 123:1071–1074
  25. Sullivan WR, Reese LC, Fenske CW (1980) Unified method for analysis of laterally loaded piles in clay. In: Numerical methods in offshore piling. Thomas Telford Publishing, pp 135–146
  26. Poulos HG (2018) Rational assessment of modulus of subgrade reaction. Geotech Eng J SEAGS AGSSEA 49:1–7
  27. Reese LC, Cox WR, Koop FD (1974) Analysis of laterally loaded piles in sand. In: Offshore Technology Conference. OnePetro
  28. Cox WR, Reese LC, Grubbs BR (1974) Field testing of laterally loaded piles in sand. In: Offshore Technology Conference. OnePetro
  29. Gao F, Li J, Qi W, Hu C (2015) On the instability of offshore foundations: theory and

- 770 mechanism. Sci China Physics, Mech Astron 58:124701.  
 771 <https://doi.org/10.1007/s11433-015-5745-9>
- 772 30. Jaky J (1948) Pressure in silos. In: Proceedings of the 2nd International Conference on  
 773 Soil Mechanics and Foundation Engineering ICSMFE. London, pp 103–107
- 774 31. Hansen B (1961) A general formula for bearing capacity. Danish Geotech Institute, Bull  
 775 11:38–46
- 776 32. Hansen JB (1970) A revised and extended formula for bearing capacity
- 777 33. Scott RF (1980) Analysis of centrifuge pile tests; simulation of pile-driving
- 778 34. Bogard D, Matlock H (1980) Simplified calculation of  $p_y$  curves for laterally loaded  
 779 piles in sand. Earth Technol Corp Inc, Houst
- 780 35. Goodno BJ, Gere JM (2020) Mechanics of materials. Cengage Learning
- 781 36. Mayne PW, Kulhawy FH (1982)  $K_0$ -OCR relationships in soil. J Geotech Eng 108  
 782 (GT6):851–872
- 783 37. Tomlinson M, Woodward J (2015) Pile design and construction practice, 6th editio.  
 784 CRC press, New York, NY  
 785  
 786